Disorder, Low-Energy Excitations, and Topology in the Kitaev Spin Liquid

Vitor Dantas and Eric C. Andrade
Instituto de Física de São Carlos, Universidade de São Paulo, C.P. 369, São Carlos, SP 13560-970, Brazil

(Received 11 January 2022; accepted 23 June 2022; published 13 July 2022)

The Kitaev model is a fascinating example of an exactly solvable model displaying a spin-liquid ground state in two dimensions. However, deviations from the original Kitaev model are expected to appear in real materials. In this Letter, we investigate the fate of Kitaev's spin liquid in the presence of disorder—bond defects or vacancies—for an extended version of the model. Considering static flux backgrounds, we observe a power-law divergence in the low-energy limit of the density of states with a nonuniversal exponent. We link this power-law distribution of energy scales to weakly coupled droplets inside the bulk, in an uncanny similarity to the Griffiths phase often present in the vicinity of disordered quantum phase transitions. If time-reversal symmetry is broken, we find that power-law singularities are tied to the destruction of the topological phase of the Kitaev model in the presence of bond disorder alone. However, there is a transition from this topologically trivial phase with power-law singularities to a topologically nontrivial one for weak to moderate site dilution. Therefore, diluted Kitaev materials are potential candidates to host Kitaev's chiral spin-liquid phase.

DOI: 10.1103/PhysRevLett.129.037204

Introduction.—Over the past decades, strong spin-orbit coupling has been recognized as a key ingredient in stabilizing unconventional phases in correlated materials [1–4]. For $4d$ and $5d$ Mott insulators, for instance, there is great interest in the Kitaev materials, which are systems hosting dominant Ising-like bond-dependent interactions for local effective moments $j_{\mathrm{eff}} = 1/2$ in stacked honeycomb planes [5–12]. If these bond-dependent interactions have similar strength, Kitaev exactly established the existence of a quantum spin liquid [13–15] of gapless Majorana fermions moving in a static $\mathbb{Z}_2$ flux background. Remarkably, an infinitesimally small external magnetic field generates chiral Majorana edge modes with half-quantized thermal Hall conductance [5,16].

A promising Kitaev material is α-$RuCl_3$ [17–19], which displays long-ranged magnetic order at low T, suggesting further magnetic interactions beyond Kitaev's [20]. The magnetic order is suppressed by an external magnetic field [21–27], and it is replaced by an intermediary phase—distinct from the high-field polarized state—that exhibits a half-quantized thermal Hall conductance [28,29].

Another putative Kitaev material is $H_3LiIr_2O_6$ [30], which shows no magnetic order down to 50 mK, making it a prominent candidate to realize Kitaev's spin-liquid phase. However, the experimental observations are at odds with the thermodynamic behavior of the clean Kitaev model [31–33]: (i) the specific heat diverges at low T as $C/T \propto T^{-1/2}$; (ii) the uniform magnetic susceptibility shows a similar, albeit milder, divergence $\chi \sim T^{-1/2}$; (iii) the $1/T_1$ NMR spin-relaxation rate has a nonvanishing contribution down to low T, and the Knight shift is almost flat in this region. All these results point to an appreciable amount of low-energy excitations.

This work shows that the experimental observations in $H_3LiIr_2O_6$ can be understood within Kitaev's model if one considers the presence of defects. Microscopic sources of the disorder include stacking faults [34] and the random position of the H ions. To study the effects of uncorrelated quenched disorder in this model in a controlled fashion, we address the role of bond disorder and site dilution (vacancies) separately.

Following the previous studies of Refs. [35,36], we also observe that a finite concentration of defects generically leads to a power-law divergence in the low-energy density of states (DOS). Motivated by this robust result, we then construct a comprehensive Griffiths-like scenario [37–41] and establish that (i) the DOS power-law exponent α is nonuniversal; (ii) C/T and χ diverge with the same exponent α; (iii) there is a nontrivial scaling for C/T when $T/B \ll 1$; and (iv) $1/T_1T$ follows a Korringa-like law. All these findings are in accordance with the experimental results for $H_3LiIr_2O_6$. Importantly, this scenario does not rely on the formation of random singlets [42–48], which is a topologically trivial state, unlike a disordered Kitaev spin liquid [49,50]. For bond disorder, however, robust power-law singularities at low magnetic fields are linked to the destruction of the topological phase. For vacancies, we find that Kitaev's chiral spin-liquid phase survives up to a critical dilution, due to a nontrivial flux configuration, before being replaced by a topologically trivial phase with power-law singularities. This suggests that a half-quantized thermal Hall conductance might be detected experimentally in diluted Kitaev materials [51–54].

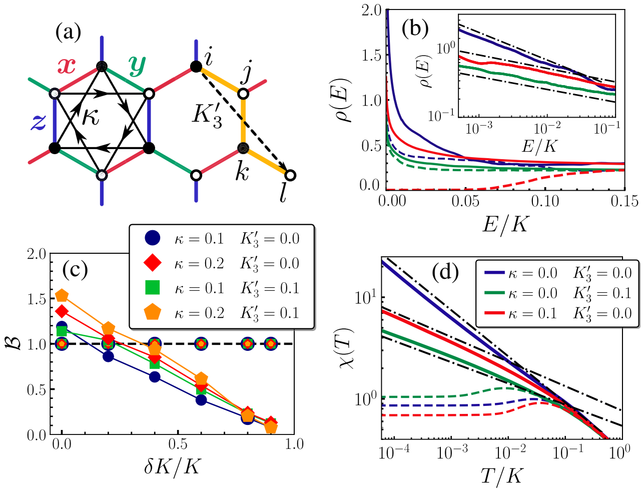

FIG. 1. Extended Kitaev model in Eq. (2) in the presence of bond disorder. (a) Links x, y, and z in the honeycomb lattice and the hopping between second (κ) and third neighbors (K_3'). (b) DOS as function of the energy for $\delta K = 0.8$. Inset: log-log plot showing the power-law divergence at low E. (c) Bott index as a function of disorder. (d) Static uniform spin susceptibility as a function of the temperature in a log-log plot for $\delta K = 0.8$. In (b)–(d) full (dashed) curves correspond to random (0) flux. We consider the same parameters in (b) and (d). The dot dashed curves in (b) and (d) are power-law fits, shifted with respect to the original curves, with $\alpha = 0.455(5), 0.222(3), 0.209(4)$. We considered $L = 30$ and 3×10^3 realizations of disorder.

Extended Kitaev model.—As a minimal model to capture the low-energy physics of $H_3LiIr_2O_6$, we consider an extended Kitaev model on the honeycomb lattice [55]:

$$\mathcal{H} = K\sum_{\langle ij\rangle_\alpha}\sigma_i^\alpha\sigma_j^\alpha + \kappa\sum_{\langle\langle ik\rangle\rangle}\sigma_i^\alpha\sigma_j^\beta\sigma_k^\gamma - K_3'\sum_{\langle\langle\langle il\rangle\rangle\rangle}\sigma_i^\alpha\sigma_j^\gamma\sigma_k^\gamma\sigma_l^\alpha, \qquad (1)$$

where K is the usual Kitaev coupling and σ_i^α is the Pauli matrix at site i with spin component $\{\alpha,\beta,\gamma\} \in \{x,y,z\}$. $\langle ij\rangle_\alpha$ labels the nearest-neighbor sites i and j along one of the three different links; see Fig. 1(a). The three-spin term mimics the effects of an external magnetic field and breaks time-reversal symmetry, with $\kappa \propto h_x h_y h_z/\Delta_{2f}$, where Δ_{2f} is the two-flux gap (to be defined below) [5]. The four-spin interaction runs along a path of length 3; see Fig. 1(a). While the K_3' term can be generated perturbatively if one includes exchange couplings beyond the pure Kitaev [56], we consider Eq. (1) as an effective low-energy theory [57], and treat K_3' as one of the first allowed terms in the theory that preserves time-reversal symmetry [55]. To restrict the model's parameter space, we consider $K, \kappa, K_3' > 0$.

Equation (1) is still amenable to the Kitaev's exact solution [5]. We write the spin operator in terms of four Majorana fermions $\sigma_j^\alpha = ib_j^\alpha c$, and the Hamiltonian becomes

$$\mathcal{H} = -iK\sum_{\langle ij\rangle_\alpha}u_{ij}^\alpha c_i c_j - i\kappa\sum_{\langle\langle ik\rangle\rangle}u_{ij}^\alpha u_{kj}^\beta c_i c_k, + iK_3'\sum_{\langle\langle\langle il\rangle\rangle\rangle}u_{ij}^\alpha u_{kj}^\beta u_{kl}^\alpha c_i c_i, \qquad (2)$$

where $u_{ij}^\alpha = -u_{ji}^\alpha = ib_i^\alpha b_j^\alpha = \pm 1$ is a conserved $\mathbb{Z}_2$ gauge field along the α bond $\langle ij\rangle_\alpha$. The flux around each hexagonal plaquette p is a conserved quantity and may be written as $W_p = \prod_{\langle ij\rangle \in p} u_{ij}^\alpha$ [5]. Since the fluxes commute with each other and with the Hamiltonian in Eq. (2), once we fix the link variable u_{ij}^α at each bond, thus defining a flux sector, the problem can be solved exactly as a tight-binding model of Majorana fermions and we obtain $\mathcal{H} = \sum_\nu (E_\nu - 1/2) f_\nu^\dagger f_\nu$. The operators f_ν are complex fermions operators (consisting in the superposition of two Majorana operators [58]) that label the eigenstate with energy E_ν in a given flux sector.

For the pure Kitaev model, $\kappa = K_3' = 0$, in the absence of disorder, we have a 0-flux ground state, i.e., $W_p = +1$ for all plaquettes. The two-flux gap is the difference between the ground state energies of a system with a single flipped link variable and the original reference state because a single bond flip creates a pair of fluxes in neighboring hexagons [5,61]. The ground state flux state depends on K_3' [55]. For our parameter regime, we find that for $K_3' \gtrsim K/8$ the ground state comprises one flux per plaquette, i.e., $W_p = -1$ for all plaquettes [58], but we do not explore this transition in this work. We consider finite clusters of linear size L, with periodic boundary conditions. Because we have two sites per unit cell, the total number of sites is $N = 2L^2$.

Bond disorder and random flux.—We now add disorder to the model in Eq. (2). Specifically, we consider a binary bond disorder for all Kitaev couplings setting $K \to K \pm \delta K$, with probability 0.5 to generate either a weak bond, $(K - \delta K)$, or a strong bond, $(K + \delta K)$. For simplicity, we assume the couplings κ and K_3' to be homogenous. In terms of Majorana fermions, this problem translates into a random hopping problem in a bipartite lattice. For $\kappa = K_3' = 0$, it is rigorously known that the DOS, $\rho(E) = \sum_\nu \delta(E - E_\nu)/N$, has a low-$E$ divergence $\rho(E) \sim \exp(-c|\ln E|^{2/3})/E$, where c is a positive constant [62,63]. Nevertheless, this divergence occurs only at asymptotically low-energy scales, eluding even large-scale numerical simulations [62,63]. This fact probably places it outside the experimentally accessible regimes for magnetic materials.

After fixing the flux state, we numerically diagonalize Eq. (2). We find that the static flux configuration is sensitive to strong disorder [64]. Specifically, we observe that for $\delta K \gtrsim 0.6$ the ground state energies of the different flux sectors become comparable within the error bars [58]. This implies that $\Delta_{2f} \to 0$ as $\delta K \to 1$, as in recent quantum Monte Carlo results [50,65]. Therefore, we consider the random flux background a competitive variational flux state. In this state, we randomly set $u_{ij}^{\alpha} = \pm 1$ at each link with equal probability.

Figure 1(b) shows the averaged DOS for $\delta K = 0.8$. For $K_3' = \kappa = 0$, both the 0-flux and random-flux states produce a diverging power-law behavior at low E: $\rho(E) \sim E^{-\alpha}$, in accordance with the results of Refs. [35,36]. If one assumes that the flux degrees of freedom are frozen, it follows that $C/T \sim T^{-\alpha}$ [35,36]. The power-law exponent α is nonuniversal and it depends continuously on the model parameters; see Fig. 1(b) [58]. The evolution of α with κ is particularly sensitive to the flux sector. While the random-flux sector experiences a reduction of α as κ increases, the 0-flux state displays a gap in the Majorana spectrum. This gap is reminiscent of the topological gap present in the clean case [5].

To further explore the effects of bond disorder on the thermodynamic response, we also calculate the static uniform susceptibility employing the adiabatic approximation [58,61,66,67]. We show sample results for $\kappa = K_3' = 0$ and $\delta K = 0.8$ in Fig. 1(d). The random-flux sector shows a diverging susceptibility $\chi \sim T^{-\alpha}$ at low T, with α the DOS exponent, in line with the results for $H_3LiIr_2O_6$ [30]. The 0-flux state, on the other hand, shows a finite χ at low T. We can trace back these behaviors to the value of Δ_{2f}. In the 0-flux state, Δ_{2f} remains finite, albeit smaller, for $\delta K > 0$ [65,68], and the susceptibility goes to a constant for $T < \Delta_{2f}$. In the random-flux state, $\Delta_{2f} \to 0$ and $\chi(T)$ follows $\rho(E)$ at low energies.

These two flux states also manifest differently in the topological properties of the system; see Fig. 1(c). To capture a nontrivial topological phase, we compute the Bott index, which is equivalent to the Chern number in periodic systems. Still, it is more conveniently implemented in systems lacking translational invariance [58,69–71]. The 0-flux state shows a stable topological phase up to $\delta K \to 1$ due to the finite topological gap in the Majorana spectrum present in $\rho(E)$ [50,68]. This is similar to what is observed in disordered two-dimensional disordered Chern insulators [72–75]. However, there is a pileup of low-energy states in the random-flux state, even for $\delta K = 0$, and the topological phase is destroyed for all δK. We complement the Bott index results with an investigation of the level spacing statistics [58,73,76,77], and the results are entirely consistent.

Based on our results, we construct the following scenario for disordered Kitaev materials. Taking κ to mimic the effects of an external magnetic field, the experimental results observed in $H_3LiIr_2O_6$ [30] can be described by Eq. (2), augmented by bond disorder, only if one assumes a random-flux state [35,36]. This, in turn, implies that power-law singularities at zero fields are associated with a topologically trivial phase in a finite field also displaying power-law singularities but with a smaller exponent.

Griffiths-like response.—We now present a physical mechanism behind the power-law singularities in the DOS. Although this is a crossover regime [62,63], the fact that it emerges for distinct choices of disorder distributions [35,36] suggests a more general picture.

Power-law distribution of energy scales is commonly observed in the vicinity of quantum critical points in disordered systems [37–41], in the so-called Griffiths phase. We exploit this similarity and propose the following mechanism. Suppose a rare region (droplet) of linear size ℓ contains only weak bonds at its boundaries. The probability of finding such cluster inside the bulk is $P(\ell) \propto \exp[b \ln(p) \ell]$, where p is the probability of finding a single weak bond and $b > 0$ is a constant. For a completely disconnected region, $\delta K \to K$, a finite-size gap appears in the Majorana spectrum $\Delta(\ell) \propto \exp[-a\ell]$, with $a > 0$ another constant. This gap comes from the hybridization of the localized states at the edges of this cluster [58]. The contribution to the density of states coming from these rare regions is $\rho(E) = \int d\ell P(\ell) \delta[E - \Delta(\ell)] \sim E^{-\alpha}$, with $\alpha = 1 + (b/a) \ln(p)$. Therefore, weakly coupled clusters give rise to a power-law singularity in the DOS. For even lower temperatures, we eventually flow away from this crossover regime toward the asymptotic result $\rho(E) \sim \exp(-c|\ln E|^{2/3})/E$ [62,63].

We extend this Griffiths phase analogy and calculate the leading low-T contribution to several physical observables in the limit of frozen flux configurations, such that we can link the spin excitations solely to $\rho(E)$. For instance, we can estimate the number of free clusters as $n(T) \sim \int_0^T \rho(E) dE \sim T^{-\alpha+1}$. This leads to a finite low-T entropy for the spins $S \sim n(T) \ln 2$ and thus $C/T \sim T^{-\alpha}$. Analogously, the uniform spin susceptibility can be estimated as $\chi(T) \sim n(T)/T \sim T^{-\alpha}$, which eventually overcomes any regular contribution from the bulk. Importantly, this result does not rely on the adiabatic approximation. The imaginary part of the dynamical susceptibility is given by $\chi''(\omega) \sim \int \delta(\omega - E) \rho(E) dE \sim \omega^{-\alpha}$. Because the cluster excitations are essentially local, we may write the NMR spin-relaxation rate $1/T_1$ as [78] $1/T_1 T \sim \chi''(\omega_o)/\omega_o \sim \omega_o^{-\alpha-1}$, where ω_o is the nuclear resonance frequency. Therefore, $1/T_1 T$ remains finite down to very low temperatures. Lastly, we can also discuss the curious data scaling encountered in Ref. [30]: $C/T \sim B^{-3/2} T$ for $T < B$, where B is the magnetic field. First, we write [5] $\kappa \sim B^3/\Delta_{2f}^2 \sim B^3/T^2$, setting T as the low-energy scale in this regime. Because $T \ll \kappa$, we employ a Sommerfeld-like expansion and write $C \sim \rho(\kappa) T \sim \kappa^{-\alpha} T \sim B^{-3\alpha} T^{1+2\alpha}$. For $\alpha = 1/2$, we obtain the experimentally observed scaling.

Therefore, a disordered extension of Kitaev's spin liquid provides a consistent scenario to the experimental results observed in $H_3LiIr_2O_6$ once we combine a power-law low-energy DOS with standard Griffiths-like arguments. However, such a scenario is incompatible with a topological nontrivial phase for bond disorder alone because it requires a random-flux state.

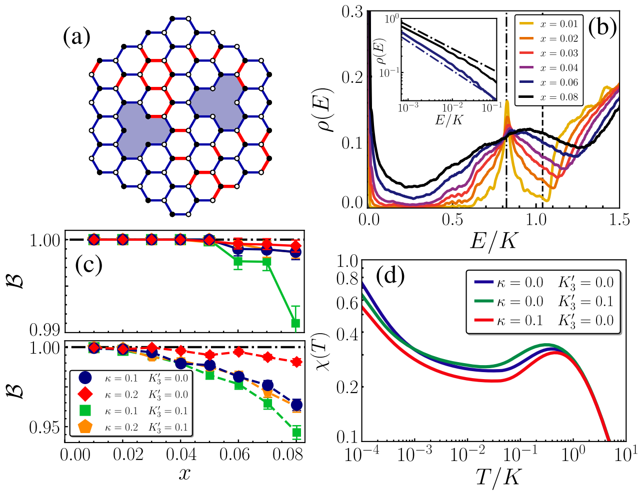

FIG. 2. Diluted extended Kitaev model, Eq. (2). (a) Bound-state flux configuration. The shaded $l = 12$ plaquettes show the binding of a flux by each vacancy. (b) DOS as function of the energy for $\kappa = 0.1K$ and $K_3' = 0$. Inset: log-log plot showing the power-law divergence at low E for $x \geq 0.06$. The dot-dashed curves are power-law fits, shifted with respect to the original curves, with $\alpha = 0.496(1), 0.445(3)$. (c) Bott index as a function of the dilution for the bound flux (0 flux) in the upper (lower) panel. (d) Log-log plot of $\chi \times T$ in the bound-flux sector for $x = 0.04$. We use the same parameters as in Fig. 1.

Site dilution and unpaired spins.—We now introduce vacancies in the extended Kitaev model, Eq. (2). Specifically, we remove a fraction x of spins from the system. To avoid trivial zero-energy modes, we remove exactly $xN/2$ spins from each sublattice. In the limit $x \ll 1$, a vacancy binds a flux to it [79]: as one loops the impurity plaquette, $W_p = -1$; see Fig. 2(a). Because we work at finite x, we consider both 0-flux and bound-flux states [36]. In the 0 (bound) flux, $W_p = +1(-1)$ in the vacancy plaquette. For all other honeycomb loops, $W_p = +1$; see Fig. 2(a). We find that the random-flux state is not a competitive ground state for $x \lesssim 0.1$ [58].

Unlike the bond disordered case, a small dilution is sufficient to induce a pileup of low-energy states, similar to what is observed in graphene [80–82], independently of the flux sector [36,58]. A clearer distinction between the different flux configurations emerges for $\kappa \neq 0$. In Fig. 2(b) we show the DOS for the bound-flux state, $\kappa = 0.1K$, $K_3' = 0$, and several values of dilution x. For $x \lesssim 0.05$, we observe a localized level inside the clean gap. The larger the κ, the more well-defined this state is. As we increase x, we reduce the impurity distance—its typical value scales as $1/\sqrt{x}$—enhancing the overlap between the impurity states, which gives rise to an impurity band inside the clean topological gap, similar to what is observed in disordered Chern insulators [72,73,75]. The resulting phase is a topologically trivial phase with power-law singularities. See the inset of Fig. 2(b).

To see the effects of the in-gap states on the topological properties of the system, we compute the Bott index; see Fig. 2(c). In the small κ regime, $\mathcal{B}$ is no longer quantized for the 0-flux state if $x > 0.02$. For the bound-flux state, however, $\mathcal{B}$ remains pinned to an integer up to $x \approx 0.05$ (this critical value depends on κ [58]). In both cases, the clean topological gap is the same, and this extra robustness of the bound-flux state is rooted in the in-gap state at finite energy shown in Fig. 2(b). The existence of this state can be understood as follows. Consider the impurity plaquette as a $l = 12$ tight-binding chain with nearest-neighbor hopping only (the vacancy plaquette has a length $l = 12$ rather than $l = 6$ for the elementary honeycomb one). The spectrum of this problem has (does not have) a gap if the chain binds (does not bind) a flux. For finite x, the impurity states go into this level, ensuring the localization of the impurity states around the vacancy for small x. For larger concentrations, other impurities configurations become relevant, e.g., a pair of neighboring vacancies [58], and more states inside the topological gap are populated. This suggests that a topological phase could be stable in the diluted system for an external field that is large enough to quantize $\mathcal{B}$ for a given x, but not too large as to move the system away from the bound-flux state [36,79]. The presence of this topological phase might be probed experimentally using the thermal Hall conductance [28,29,83]. Despite being challenging, these measurements could be relevant both to $H_3LiIr_2O_6$ [30] and Ir-doped $RuCl_3$ [52–54].

In Fig. 2(d), we show sample results for the static uniform spin susceptibility $\chi(T)$. We observe a mild increase in $\chi(T)$ for the bound flux, with similar results for the 0 flux. A bona fide power-law divergence is present only at much lower temperatures [58]. This behavior is due to the existence of unpaired bonds [65]. By removing a site, we automatically leave its three nearest neighbors disconnected along one bond. Such unpaired bonds automatically display $\Delta_{2f} = 0$, and they dominate the low-T behavior of $\chi(T)$. However, since the fraction of unpaired spins is equal to x, at least for small x, their overall contribution is masked by the remaining $1 - x$ fraction of bulk spins that give a finite contribution to $\chi(T)$ if $T < \Delta_{2f}$ [58]. This is also in line with the Knight shift measurements reported in [30]: spins far away from the defects produce a regular flat contribution to the local spin susceptibility, whereas spins around a vacancy give a singular response. Because the condition $\Delta_{2f} = 0$ is automatically satisfied by these unpaired spins, the Griffiths-like arguments discussed previously apply directly here, regardless of the considered static flux background. As a closing remark, we stress that the asymptotic results for $\chi(T)$ calculated in Ref. [79] are only relevant for large fields, where the magnetic length is smaller than the typical interimpurity distance, and the single vacancy limit holds.

Conclusions.—We investigated an extended Kitaev model, Eq. (2), in the presence of defects. We find the emergence of a singular power-law density of states at low energies [35,36] with a nonuniversal exponent. We then construct a phenomenological scenario for our numerical findings by discussing this power-law distribution of energy scales in terms of a Griffiths-like phase. Our results provide a consistent scenario to the experimental observations for $H_3LiIr_2O_6$ [30], and we expect them to describe other diluted Kitaev materials as $RuCl_3$ [52–54] and the Iridates [51,84].

From a theoretical perspective, this unanticipated link deserves further study since a Griffiths-like phenomenology appears naturally in a random-singlet phase [42–48]. In the absence of disorder, a valence-bond crystal and the Kitaev spin liquid are separated by a quantum phase transition [85,86]. Our work points toward an exciting evolution of this critical point with the disorder.

In the presence of a time-reversal breaking term, we find that the topological properties of the system are sensitive both to the static flux background and to the particular choice of disorder. For bond disorder, the power-law singularities are robust only if one assumes a random-flux background, implying a lack of a topological spin-liquid phase. However, the power-law singularities survive at weak external magnetic fields for small concentrations of vacancies. They are eventually quenched at larger fields, where a topological phase with chiral Majorana edge modes emerges. The stability of this topological phase comes from the fact that a vacancy binds a flux to it, which helps protect the clean topological gap in the Majorana spectrum. Our results indicate that diluted Kitaev materials are promising candidates to display Kitaev's chiral spin-liquid phase in weak to moderate magnetic fields.

We acknowledge useful discussions with Pedro Cônsoli, José Hoyos, Lukas Janssen, Eduardo Miranda, João Augusto Sobral, and Matthias Vojta. V. D. acknowledges the support from the University of São Paulo. E. C. A. was supported by CNPq (Brazil), Grants No. 406399/2018-2 and 302994/2019-0, and FAPESP (Brazil), Grant No. 2019/17026-9.

[1] G. Khaliullin, Orbital order and fluctuations in Mott insulators, Prog. Theor. Phys. Suppl. **160**, 155 (2005).
[2] W. Witczak-Krempa, G. Chen, Y. B. Kim, and L. Balents, Correlated quantum phenomena in the strong spin-orbit regime, Annu. Rev. Condens. Matter Phys. **5**, 57 (2014).
[3] Z. Nussinov and J. van den Brink, Compass models: Theory and physical motivations, Rev. Mod. Phys. **87**, 1 (2015).
[4] J. G. Rau, E. K.-H. Lee, and H.-Y. Kee, Spin-orbit physics giving rise to novel phases in correlated systems: Iridates and related materials, Annu. Rev. Condens. Matter Phys. **7**, 195 (2016).
[5] A. Kitaev, Anyons in an exactly solved model and beyond, Ann. Phys. (N.Y.) **321**, 2 (2006).
[6] G. Jackeli and G. Khaliullin, Mott Insulators in the Strong Spin-Orbit Coupling Limit: From Heisenberg to a Quantum Compass and Kitaev Models, Phys. Rev. Lett. **102**, 017205 (2009).
[7] J. Chaloupka, G. Jackeli, and G. Khaliullin, Kitaev-Heisenberg Model on a Honeycomb Lattice: Possible Exotic Phases in Iridium Oxides A_2IrO_3, Phys. Rev. Lett. **105**, 027204 (2010).
[8] J. Chaloupka, G. Jackeli, and G. Khaliullin, Zigzag Magnetic Order in the Iridium Oxide Na_2IrO_3, Phys. Rev. Lett. **110**, 097204 (2013).
[9] S. M. Winter, A. A. Tsirlin, M. Daghofer, J. van den Brink, Y. Singh, P. Gegenwart, and R. Valentí, Models and materials for generalized Kitaev magnetism, J. Phys. Condens. Matter **29**, 493002 (2017).
[10] S. Trebst, Kitaev materials, arXiv:1701.07056.
[11] M. Hermanns, I. Kimchi, and J. Knolle, Physics of the Kitaev model: Fractionalization, dynamic correlations, and material connections, Annu. Rev. Condens. Matter Phys. **9**, 17 (2018).
[12] H. Takagi, T. Takayama, G. Jackeli, G. Khaliullin, and S. E. Nagler, Concept and realization of Kitaev quantum spin liquids, Nat. Rev. Phys. **1**, 264 (2019).
[13] L. Balents, Spin liquids in frustrated magnets, Nature (London) **464**, 199 (2010).
[14] L. Savary and L. Balents, Quantum spin liquids: A review, Rep. Prog. Phys. **80**, 016502 (2017).
[15] C. Broholm, R. J. Cava, S. A. Kivelson, D. G. Nocera, M. R. Norman, and T. Senthil, Quantum spin liquids, Science **367**, eaay0668 (2020).
[16] C. Hickey and S. Trebst, Emergence of a field-driven U(1) spin liquid in the Kitaev honeycomb model, Nat. Commun. **10**, 530 (2019).
[17] K. W. Plumb, J. P. Clancy, L. J. Sandilands, V. V. Shankar, Y. F. Hu, K. S. Burch, H.-Y. Kee, and Y.-J. Kim, α-$RuCl_3$: A spin-orbit assisted Mott insulator on a honeycomb lattice, Phys. Rev. B **90**, 041112(R) (2014).
[18] J. A. Sears, M. Songvilay, K. W. Plumb, J. P. Clancy, Y. Qiu, Y. Zhao, D. Parshall, and Y.-J. Kim, Magnetic order in α-$RuCl_3$: A honeycomb-lattice quantum magnet with strong spin-orbit coupling, Phys. Rev. B **91**, 144420 (2015).
[19] A. Banerjee, C. A. Bridges, J.-Q. Yan, A. A. Aczel, L. Li, M. B. Stone, G. E. Granroth, M. D. Lumsden, Y. Yiu, J. Knolle, S. Bhattacharjee, D. L. Kovrizhin, R. Moessner, D. A. Tennant, D. G. Mandrus, and S. E. Nagler, Proximate Kitaev quantum spin liquid behaviour in a honeycomb magnet, Nat. Mater. **15**, 733 (2016).
[20] L. Janssen, E. C. Andrade, and M. Vojta, Magnetization processes of zigzag states on the honeycomb lattice: Identifying spin models for α-$RuCl_3$ and Na_2IrO_3, Phys. Rev. B **96**, 064430 (2017).
[21] J. A. Sears, Y. Zhao, Z. Xu, J. W. Lynn, and Y.-J. Kim, Phase diagram of α-$RuCl_3$ in an in-plane magnetic field, Phys. Rev. B **95**, 180411(R) (2017).
[22] A. U. B. Wolter, L. T. Corredor, L. Janssen, K. Nenkov, S. Schönecker, S.-H. Do, K.-Y. Choi, R. Albrecht, J. Hunger, T. Doert, M. Vojta, and B. Büchner, Field-induced quantum criticality in the Kitaev system α-$RuCl_3$, Phys. Rev. B **96**, 041405(R) (2017).
[23] Y. Kasahara, K. Sugii, T. Ohnishi, M. Shimozawa, M. Yamashita, N. Kurita, H. Tanaka, J. Nasu, Y. Motome, T. Shibauchi, and Y. Matsuda, Unusual Thermal Hall Effect in a Kitaev Spin Liquid Candidate α-$RuCl_3$, Phys. Rev. Lett. **120**, 217205 (2018).

[24] L. Janssen and M. Vojta, Heisenberg-Kitaev physics in magnetic fields, J. Phys. Condens. Matter **31**, 423002 (2019).

[25] C. Balz, P. Lampen-Kelley, A. Banerjee, J. Yan, Z. Lu, X. Hu, S. M. Yadav, Y. Takano, Y. Liu, D. A. Tennant, M. D. Lumsden, D. Mandrus, and S. E. Nagler, Finite field regime for a quantum spin liquid in α-$RuCl_3$, Phys. Rev. B **100**, 060405(R) (2019).

[26] S. Gass, P. M. Cônsoli, V. Kocsis, L. T. Corredor, P. Lampen-Kelley, D. G. Mandrus, S. E. Nagler, L. Janssen, M. Vojta, B. Büchner, and A. U. B. Wolter, Field-induced transitions in the Kitaev material α-$RuCl_3$ probed by thermal expansion and magnetostriction, Phys. Rev. B **101**, 245158 (2020).

[27] P. M. Cônsoli, L. Janssen, M. Vojta, and E. C. Andrade, Heisenberg-Kitaev model in a magnetic field: $1/S$ expansion, Phys. Rev. B **102**, 155134 (2020).

[28] Y. Kasahara, T. Ohnishi, Y. Mizukami, O. Tanaka, S. Ma, K. Sugii, N. Kurita, H. Tanaka, J. Nasu, Y. Motome, T. Shibauchi, and Y. Matsuda, Majorana quantization and half-integer thermal quantum Hall effect in a Kitaev spin liquid, Nature (London) **559**, 227 (2018).

[29] T. Yokoi, S. Ma, Y. Kasahara, S. Kasahara, T. Shibauchi, N. Kurita, H. Tanaka, J. Nasu, Y. Motome, C. Hickey, S. Trebst, and Y. Matsuda, Half-integer quantized anomalous thermal Hall effect in the Kitaev material candidate α-$RuCl_3$, Science **373**, 568 (2021).

[30] K. Kitagawa, T. Takayama, Y. Matsumoto, A. Kato, R. Takano, Y. Kishimoto, S. Bette, R. Dinnebier, G. Jackeli, and H. Takagi, A spin–orbital-entangled quantum liquid on a honeycomb lattice, Nature (London) **554**, 341 (2018).

[31] J. Nasu, M. Udagawa, and Y. Motome, Vaporization of Kitaev Spin Liquids, Phys. Rev. Lett. **113**, 197205 (2014).

[32] J. Nasu, M. Udagawa, and Y. Motome, Thermal fractionalization of quantum spins in a Kitaev model: Temperature-linear specific heat and coherent transport of Majorana fermions, Phys. Rev. B **92**, 115122 (2015).

[33] K. Feng, N. B. Perkins, and F. J. Burnell, Further insights into the thermodynamics of the Kitaev honeycomb model, Phys. Rev. B **102**, 224402 (2020).

[34] L. R. D. Freitas and R. G. Pereira, Gapless excitations in non-abelian kitaev spin liquids with line defects, Phys. Rev. B **105**, L041104 (2022).

[35] J. Knolle, R. Moessner, and N. B. Perkins, Bond-Disordered Spin Liquid and the Honeycomb Iridate $H_3LiIr_2O_6$: Abundant Low-Energy Density of States from Random Majorana Hopping, Phys. Rev. Lett. **122**, 047202 (2019).

[36] W.-H. Kao, J. Knolle, G. B. Halász, R. Moessner, and N. B. Perkins, Vacancy-Induced Low-Energy Density of States in the Kitaev Spin Liquid, Phys. Rev. X **11**, 011034 (2021).

[37] E. Miranda and V. Dobrosavljević, Disorder-driven non-Fermi liquid behaviour of correlated electrons, Rep. Prog. Phys. **68**, 2337 (2005).

[38] T. Vojta, Rare region effects at classical, quantum and nonequilibrium phase transitions, J. Phys. A **39**, R143 (2006).

[39] E. C. Andrade, E. Miranda, and V. Dobrosavljević, Electronic Griffiths Phase of the $d = 2$ Mott Transition, Phys. Rev. Lett. **102**, 206403 (2009).

[40] T. Vojta, Quantum Griffiths effects and smeared phase transitions in metals: Theory and experiment, J. Low Temp. Phys. **161**, 299 (2010).

[41] T. Vojta and J. A. Hoyos, Criticality and Quenched Disorder: Harris Criterion Versus Rare Regions, Phys. Rev. Lett. **112**, 075702 (2014).

[42] R. N. Bhatt and P. A. Lee, Scaling Studies of Highly Disordered Spin-$\frac{1}{2}$ Antiferromagnetic Systems, Phys. Rev. Lett. **48**, 344 (1982).

[43] S. Zhou, J. A. Hoyos, V. Dobrosavljević, and E. Miranda, Valence-bond theory of highly disordered quantum antiferromagnets, Europhys. Lett. **87**, 27003 (2009).

[44] K. Uematsu and H. Kawamura, Randomness-induced quantum spin liquid behavior in the $s = \frac{1}{2}$ random $J_1 - J_2$ Heisenberg antiferromagnet on the square lattice, Phys. Rev. B **98**, 134427 (2018).

[45] L. Liu, H. Shao, Y.-C. Lin, W. Guo, and A. W. Sandvik, Random-Singlet Phase in Disordered Two-Dimensional Quantum Magnets, Phys. Rev. X **8**, 041040 (2018).

[46] I. Kimchi, A. Nahum, and T. Senthil, Valence Bonds in Random Quantum Magnets: Theory and Application to $YbMgGaO_4$, Phys. Rev. X **8**, 031028 (2018).

[47] I. Kimchi, J. P. Sheckelton, T. M. McQueen, and P. A. Lee, Scaling and data collapse from local moments in frustrated disordered quantum spin systems, Nat. Commun. **9**, 4367 (2018).

[48] S. Sanyal, K. Damle, J. T. Chalker, and R. Moessner, Emergent Moments and Random Singlet Physics in a Majorana Spin Liquid, Phys. Rev. Lett. **127**, 127201 (2021).

[49] M. G. Yamada and S. Fujimoto, Quantum liquid crystals in the finite-field KΓ model for α-$RuCl_3$, arXiv:2107.03045.

[50] J. Nasu and Y. Motome, Thermodynamic and transport properties in disordered Kitaev models, Phys. Rev. B **102**, 054437 (2020).

[51] S. Manni, Y. Tokiwa, and P. Gegenwart, Effect of nonmagnetic dilution in the honeycomb-lattice iridates Na_2IrO_3 and Li_2IrO_3, Phys. Rev. B **89**, 241102(R) (2014).

[52] S.-H. Do, W.-J. Lee, S. Lee, Y. S. Choi, K.-J. Lee, D. I. Gorbunov, J. Wosnitza, B. J. Suh, and K.-Y. Choi, Short-range quasistatic order and critical spin correlations in α-$Ru_{1-x}Ir_xCl_3$, Phys. Rev. B **98**, 014407 (2018).

[53] S.-H. Do, C. H. Lee, T. Kihara, Y. S. Choi, S. Yoon, K. Kim, H. Cheong, W.-T. Chen, F. Chou, H. Nojiri, and K.-Y. Choi, Randomly Hopping Majorana Fermions in the Diluted Kitaev System α-$Ru_{0.8}Ir_{0.2}Cl_3$, Phys. Rev. Lett. **124**, 047204 (2020).

[54] S.-H. Baek, H. W. Yeo, S.-H. Do, K.-Y. Choi, L. Janssen, M. Vojta, and B. Büchner, Observation of a random singlet state in a diluted Kitaev honeycomb material, Phys. Rev. B **102**, 094407 (2020).

[55] S.-S. Zhang, Z. Wang, G. B. Halász, and C. D. Batista, Vison Crystals in an Extended Kitaev Model on the Honeycomb Lattice, Phys. Rev. Lett. **123**, 057201 (2019).

[56] D. Takikawa and S. Fujimoto, Topological phase transition to Abelian anyon phases due to off-diagonal exchange interaction in the Kitaev spin liquid state, Phys. Rev. B **102**, 174414 (2020).

[57] X.-Y. Song, Y.-Z. You, and L. Balents, Low-Energy Spin Dynamics of the Honeycomb Spin Liquid Beyond the Kitaev Limit, Phys. Rev. Lett. **117**, 037209 (2016).

[58] See Supplemental Material at http://link.aps.org/supplemental/10.1103/PhysRevLett.129.037204 for a detailed description of our numerical approach, as well as further results, which includes Refs. [59,60].

[59] A. Clauset, C. R. Shalizi, and M. E. J. Newman, Power-law distributions in empirical data, SIAM Rev. **51**, 661 (2009).

[60] J.-N. Fuchs, S. Patil, and J. Vidal, Parity of Chern numbers in the Kitaev honeycomb model and the sixteenfold way, Phys. Rev. B **102**, 115130 (2020).

[61] J. Knolle, D. L. Kovrizhin, J. T. Chalker, and R. Moessner, Dynamics of a Two-Dimensional Quantum Spin Liquid: Signatures of Emergent Majorana Fermions and Fluxes, Phys. Rev. Lett. **112**, 207203 (2014).

[62] O. Motrunich, K. Damle, and D. A. Huse, Particle-hole symmetric localization in two dimensions, Phys. Rev. B **65**, 064206 (2002).

[63] S. Sanyal, K. Damle, and O. I. Motrunich, Vacancy-Induced Low-Energy States in Undoped Graphene, Phys. Rev. Lett. **117**, 116806 (2016).

[64] F. Zschocke and M. Vojta, Physical states and finite-size effects in Kitaev's honeycomb model: Bond disorder, spin excitations, and NMR line shape, Phys. Rev. B **92**, 014403 (2015).

[65] J. Nasu and Y. Motome, Spin dynamics in the Kitaev model with disorder: Quantum Monte Carlo study of dynamical spin structure factor, magnetic susceptibility, and NMR relaxation rate, Phys. Rev. B **104**, 035116 (2021).

[66] G. Baskaran, S. Mandal, and R. Shankar, Exact Results for Spin Dynamics and Fractionalization in the Kitaev Model, Phys. Rev. Lett. **98**, 247201 (2007).

[67] J. Knolle, D. L. Kovrizhin, J. T. Chalker, and R. Moessner, Dynamics of fractionalization in quantum spin liquids, Phys. Rev. B **92**, 115127 (2015).

[68] M. G. Yamada, Anderson–Kitaev spin liquid, npj Quantum Mater. **5**, 82 (2020).

[69] M. B. Hastings and T. A. Loring, Topological insulators and C*-algebras: Theory and numerical practice, Ann. Phys. (Amsterdam) **326**, 1699 (2011).

[70] A. Agarwala and V. B. Shenoy, Topological Insulators in Amorphous Systems, Phys. Rev. Lett. **118**, 236402 (2017).

[71] H. Huang and F. Liu, Quantum Spin Hall Effect and Spin Bott Index in a Quasicrystal Lattice, Phys. Rev. Lett. **121**, 126401 (2018).

[72] M. Onoda, Y. Avishai, and N. Nagaosa, Localization in a Quantum Spin Hall System, Phys. Rev. Lett. **98**, 076802 (2007).

[73] E. Prodan, T. L. Hughes, and B. A. Bernevig, Entanglement Spectrum of a Disordered Topological Chern Insulator, Phys. Rev. Lett. **105**, 115501 (2010).

[74] Jose H. García, Lucian Covaci, and Tatiana G. Rappoport, Real-Space Calculation of the Conductivity Tensor for Disordered Topological Matter, Phys. Rev. Lett. **114**, 116602 (2015).

[75] E. V. Castro, M. P. López-Sancho, and M. A. H. Vozmediano, Anderson localization and topological transition in Chern insulators, Phys. Rev. B **92**, 085410 (2015).

[76] V. Oganesyan and D. A. Huse, Localization of interacting fermions at high temperature, Phys. Rev. B **75**, 155111 (2007).

[77] Y. Y. Atas, E. Bogomolny, O. Giraud, and G. Roux, Distribution of the Ratio of Consecutive Level Spacings in Random Matrix Ensembles, Phys. Rev. Lett. **110**, 084101 (2013).

[78] P. Coleman, *Introduction to Many-Body Physics* (Cambridge University Press, Cambridge, England, 2015).

[79] A. J. Willans, J. T. Chalker, and R. Moessner, Disorder in a Quantum Spin Liquid: Flux Binding and Local Moment Formation, Phys. Rev. Lett. **104**, 237203 (2010).

[80] V. M. Pereira, F. Guinea, J. M. B. Lopes dos Santos, N. M. R. Peres, and A. H. Castro Neto, Disorder Induced Localized States in Graphene, Phys. Rev. Lett. **96**, 036801 (2006).

[81] V. M. Pereira, J. M. B. Lopes dos Santos, and A. H. Castro Neto, Modeling disorder in graphene, Phys. Rev. B **77**, 115109 (2008).

[82] V. Häfner, J. Schindler, N. Weik, T. Mayer, S. Balakrishnan, R. Narayanan, S. Bera, and F. Evers, Density of States in Graphene with Vacancies: Midgap Power Law and Frozen Multifractality, Phys. Rev. Lett. **113**, 186802 (2014).

[83] P. Czajka, T. Gao, M. Hirschberger, P. Lampen-Kelley, A. Banerjee, J. Yan, D. G. Mandrus, S. E. Nagler, and N. P. Ong, Oscillations of the thermal conductivity in the spin-liquid state of α-$RuCl_3$, Nat. Phys. **17**, 915 (2021).

[84] E. C. Andrade and M. Vojta, Magnetism in spin models for depleted honeycomb-lattice iridates: Spin-glass order towards percolation, Phys. Rev. B **90**, 205112 (2014).

[85] M. Vojta, Frustration and quantum criticality, Rep. Prog. Phys. **81**, 064501 (2018).

[86] M. Majumder, R. S. Manna, G. Simutis, J. C. Orain, T. Dey, F. Freund, A. Jesche, R. Khasanov, P. K. Biswas, E. Bykova, N. Dubrovinskaia, L. S. Dubrovinsky, R. Yadav, L. Hozoi, S. Nishimoto, A. A. Tsirlin, and P. Gegenwart, Breakdown of Magnetic Order in the Pressurized Kitaev Iridate $\beta - Li_2IrO_3$, Phys. Rev. Lett. **120**, 237202 (2018).